Effects of $SrTiO_3$ capping in $La_{2/3}Ca_{1/3}MnO_3$ electrodes of different orientations

I. C. Infante,[1,a)] F. Sánchez,[1] J. Fontcuberta,[1] S. Estradé,[2] F. Peiró,[2] J. Arbiol,[2,3] M. Wojcik,[4] and E. Jedryka[4]
[1]*Institut de Ciència de Materials de Barcelona-CSIC, Campus UAB, 08193 Bellaterra, Catalonia, Spain*
[2]*EME/CeRMAE/IN2UB, Dept. d'Electrònica, Universitat de Barcelona, 08028 Barcelona, Catalonia, Spain*
[3]*TEM-MAT, Serveis Cientificotècnics, Universitat de Barcelona, 08028 Barcelona, Catalonia, Spain*
[4]*Institute of Physics, Polish Academy of Sciences, Al. Lotnikow 32/46, 02 668 Warszawa, Poland*

(Presented on 9 November 2007; received 10 September 2007; accepted 23 October 2007; published online 11 February 2008)

We report on the study of the structural, magnetic, and electronic properties of $SrTiO_3$ capped $La_{2/3}Ca_{1/3}MnO_3$ electrodes grown on (001) and (110) $SrTiO_3$ substrates. Magnetic properties of the (001) and (110) capped electrodes evolve differently when the capping layer thickness increases, revealing a reduction of the saturation magnetization for the (001) ones. Electronic properties are studied combining ^{55}Mn nuclear magnetic resonance (NMR) and x-ray photoemission spectroscopy (XPS). NMR experiments highlight that electronic phase separation in the (001) electrodes is enhanced by the presence of the $SrTiO_3$ capping layer and XPS measurements show that the electronic state of interfacial Mn ions from (001) electrode is more sensitive to the capping layer.
 [DOI: 10.1063/1.2832434]

The research on manganite materials ($R_{1-x}A_xMnO_3$, where R is a trivalent rare earth and A a divalent alkaline ion) for their integration into spintronics devices has recently received much attention. The half-metallicity of these materials makes them proper electrodes in magnetic tunnel junctions (MTJ's). Nevertheless, the usefulness of MTJ's with manganites electrodes has been found to be very limited,[1–4] showing a reduction both in the spin polarization and in the working temperature of the device compared to the maximum polarization and Curie temperature of the electrode. The reduction of the functional properties was proposed to arise from different physical phenomena occurring at the interfaces, as charge redistribution and loss of spin polarization due to electron scattering.[5,6] The majority of the reported studies of the interface phenomena were focused on the (001)-oriented heterostructures, using typically insulating $SrTiO_3$ (STO) substrates and barriers.

(110)-oriented manganite films and heterostructures have recently provided hopeful results concerning the growth on STO (110).[7–9] In particular, (110)-oriented films of the optimally doped $La_{2/3}Ca_{1/3}MnO_3$ (LCMO) present enhanced magnetic and electronic properties compared to the (001) counterparts,[9] with higher saturation magnetization, Curie temperature and no sign of phase separation. Therefore, the particularly ideal magnetic and electronic properties of the (110) electrodes and the expected less defective (110) interfaces would overcome current limitations of MTJ's.

With the aim of studying the influence of insulating capping layers on the (001) and (110)-oriented manganite electrodes, we carried out structural, magnetic, and electronic characterizations of thin LCMO electrodes and STO/LCMO heterostructures. We will show here that there is a clear reduction of the LCMO functional properties associated with the growth of insulating STO capping layers in the (001)-oriented samples, whereas (110)-oriented ones do not suffer major modifications on their properties. Consequences for the further development of MTJ's based on manganites will be discussed.

Thin films of LCMO and STO/LCMO bilayers were deposited by rf magnetron sputtering. Deposition conditions were 330 mTorr as chamber pressure (80% Ar, 20% O_2) with substrate temperature of 800 °C for (001) LCMO layers and 750 °C for (110) ones. Bilayers were prepared in a single process, performing the STO capping under the same pressure conditions as for LCMO layers and at 800 °C of substrate temperature. The thickness of LCMO electrodes was $t_{LCMO}=39$ nm and the thickness range for STO capping layers from 2 to 5 nm.

Structural properties were studied by x-ray diffraction. Reciprocal space maps (RSM's) were obtained to evaluate the unit cell parameters. Magnetic properties were measured in a commercial superconducting quantum interface device (Quantum Design). Spin echo ^{55}Mn nuclear magnetic resonance (NMR) experiments were performed at 4.2 K, in zero external magnetic field, and at several values of the excitation rf field in order to optimize the signal intensity at each frequency. NMR spectra were obtained in the frequency range of 280–450 MHz by plotting every 1 MHz an optimum spin echo signal intensity corrected for the intrinsic enhancement factor η and the frequency dependent sensitivity factor ω^2, as described in details in Ref. 10.

X-ray photoemission spectroscopy (XPS) experiments were performed using a monochromatic x-ray source (Al $K\alpha$) and setting the analyzer pass energy to be 23.5 eV. Survey spectra and the following core levels were recorded: La $3d$, Ca $2p$, Mn $2p$, Mn $3s$, Ar $2p$, and C $1s$ at 45° grazing incidence. Binding energy calibration was done by referenc-

a)Electronic mail: icanerin@icmab.es. Also at TEM-MAT, Serveis Cientificotècnics, Universitat de Barcelona, 08028 Barcelona, Spain.

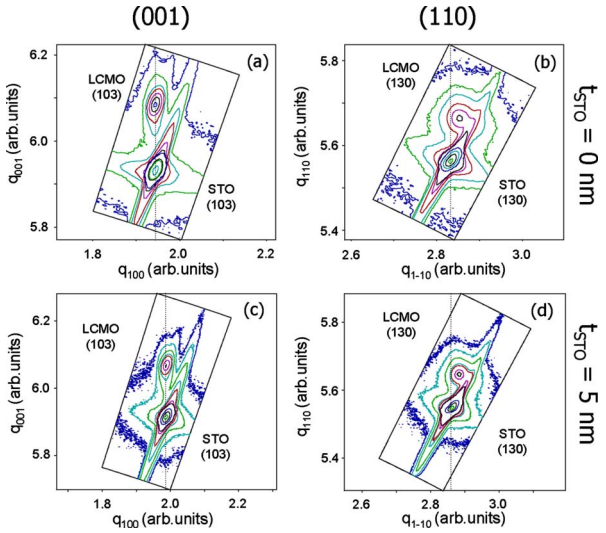

FIG. 1. (Color online) Reciprocal space maps of LCMO electrodes [(a) and (b)] and 5 nm STO capped LCMO electrodes [(c) and (d)] around the (103) reflections for (001)-oriented samples [(a) and (c)] and around the (130) reflections for (110)-oriented samples [(b) and (d)].

ing the recorded peaks to the La $3d_{5/2}$ line at 834.9 eV. Ar^+ ion etching at 4 keV (6 s) was used to remove surface contamination on bilayers.

Figure 1 shows the RSM's collected for bare (001) and (110) electrodes and 5 nm STO capped LCMO electrodes. STO substrates induce a tensile strain on the LCMO unit cell, being their corresponding cubic and pseudocubic parameters $a_{STO}=3.905$ Å and $a_{LCMO}=3.863$ Å. For the (001)-oriented samples (panels a and c) the RSM's were collected around (103) reflections and they reveal the same in-plane interplanar distance (d_{100}) for the substrate and LCMO electrode. The out-of-plane interplanar distance (d_{001}) does not appreciably change when capping with STO within the experimental limits, being the corresponding values $d_{001}=3.806$ Å (bare electrode) and $d_{001}=3.807$ Å (after 5 nm STO capping). Thus, the (001) electrode remains fully strained. For the (110)-oriented samples (panels b and d) two unequivalent in-plane orthogonal directions exist: [001] and [1−10]. We present here only the RSM's around the (130) reflections, which are used to determine the in-plane interplanar distance along the [1−10] direction (d_{1-10}). Similarly, the in-plane interplanar distance along the [001] direction is evaluated from RSM's around the (222) reflections. It is found that the in-plane interplanar distances are partially relaxed for both the bare electrode ($d_{1-10}=2.742$ Å) and the 5 nm STO capped one ($d_{1-10}=2.741$ Å) being the corresponding interplanar distance for the substrate $d_{1-10}^{STO}=2.761$ Å. The out-of-plane interplanar distance (d_{110}) is not affected by the STO capping, and the very same value is measured for both bare electrodes and capped one ($d_{110}=2.713$ Å). On the other hand, the different strain states of the (001) LCMO electrodes and (110) counterparts was previously reported[9] and originates from the different mechanical properties of the (001) and (110) planes.

The temperature dependence of magnetization of bare electrodes and 4 nm STO capped ones is shown in Fig. 2. The magnetic field (5 kOe) was applied in-plane, along the

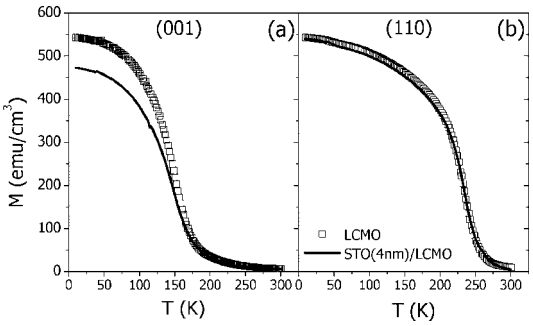

FIG. 2. Temperature dependence of the magnetization of LCMO electrodes (symbols) and 4 nm STO capped LCMO electrodes (lines): (a) (001) samples and (b) (110) samples. More details in the text.

[100] direction for the (001)-oriented samples and along the [001] one for the (110)-oriented samples. T_C of the bare electrodes (symbols) is clearly dependent on the substrate orientation, being higher for the (110) one [Fig. 2(b)] and closer to LCMO bulk value (~270 K) than for the (001) electrode [Fig. 2(a)]. T_C values of these samples are $T_{C\ 001}\sim 180$ K and $T_{C\ 110}\sim 256$ K. Upon depositing 4 nm thick capping layers (lines) the T_C of the electrodes does not change appreciably, while the magnetization of the (001) samples is clearly reduced after the capping. On the contrary, no relevant decrease on magnetization is observed for the (110) samples. From magnetization curves vs field measured at 10 K (not shown here), we have determined the saturation magnetization (M_S) of these samples, being for the bare electrodes $M_{S\ 001\text{-elect}}=543$ emu/cm^3 and $M_{S\ 110\text{-elect}}=570$ emu/cm^3, whereas for the capped electrodes $M_{S\ 001\text{-capped}}=488$ emu/cm^3 and $M_{S\ 110\text{-capped}}=548$ emu/cm^3. The reduction of M_S in capped samples accounts for a decrease on the amount of ferromagnetic Mn ions, which has to be directly correlated to the presence of the STO capping layer. The reduction of M_S in the (001) sample (10%) and in the (110) one (4%) gives an estimation of the thickness (t) of the created nonferromagnetic layer, commonly referred as dead layer, which is $t_{001}=3.9$ nm for the (001) capped electrode and $t_{110}=1.6$ nm for the (110) one. The development of dead layers in manganite film and heterostructures has been related to the substrate-induced strain as well as to the electronic interface interaction[5,9,11,12] and the exact relevance of each effect has not been definitely settled.

To get an insight into the origin of the dead layer, *ex situ* ^{55}Mn NMR and XPS experiments were performed on bare electrodes and 4 nm STO capped samples. Figure 3 shows the ^{55}Mn NMR spectra of the (001)-oriented (a) and (110)-oriented (b) samples. The dominating line corresponds to the mixed valence $Mn^{3+/4+}$ state ($\nu\sim 375$ MHz), related to averaged ^{55}Mn hyperfine field created by electron holes fast motion over manganese sites $Mn^{4+}-Mn^{3+}$. Inspection of the (001) spectra [Fig. 3(a)] reveals the presence of a broad peak at lower frequency (~315 MHz) and of smaller intensity. This secondary line is attributed to the existence of localized ferromagnetic Mn^{4+} state and thus of electronic phase separation, and it has been repetitively found in (001) manganite films grown under different conditions.[9,12,13] Moreover, the

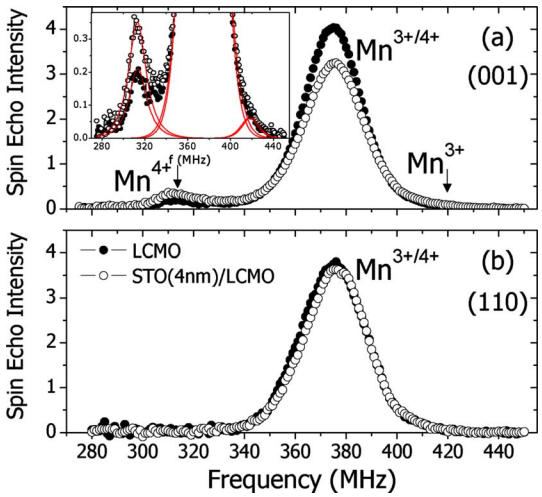

FIG. 3. (Color online) ^{55}Mn NMR spectra recorded at 4.2 K for LCMO electrodes (solid symbols) and 4 nm STO capped LCMO electrodes (open symbols): (a) (001) samples and (b) (110) samples. Inset: detail of NMR spectra of (001) samples and fits corresponding to Mn^{4+}, $Mn^{3+/4+}$, and Mn^{3+} contributions (lines).

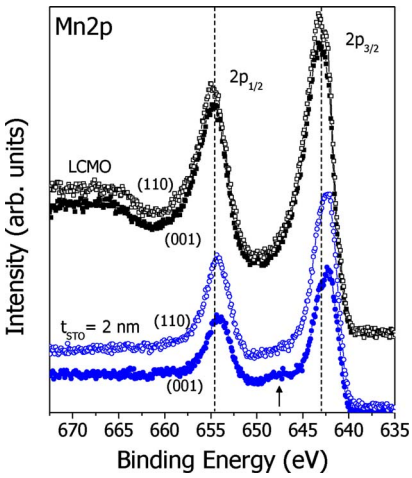

FIG. 4. (Color online) Mn $2p$ photoelectron emission spectra for LCMO electrodes (squares, top curves) and 2 nm STO capped LCMO electrodes (circles, bottom curves), with solid symbols for the (001) samples and open symbols for the (110) ones.

slight asymmetry at high frequency (~420 MHz) signals the existence of another ferromagnetic state of Mn, which corresponds to localized Mn^{+3} one.[14] However, the amount of Mn in this state does not appreciably change by the presence of a capping layer (inset) which may be due to the very fast relaxation reported for Mn^{3+} state. On the other hand, the (001) capped electrode shows a clear decrease on the intensity of the dominating $Mn^{3+/4+}$ line and an increase of the Mn^{4+} one. From the Gaussian-Lorentzian fits performed on these data (inset), we evaluate the relative amount of $Mn^{4+}/Mn^{3+/4+}$, being for the bare electrode (solid symbols) 4% and for the capped sample (open symbols) 8%. Thus, the change on the electrode dead layer associated with an increase of Mn^{4+} ions upon capping corresponds to $t_{001} \sim 1.5$ nm. In general, charge localization implies weakening of the double exchange coupling, as already seen from magnetization curves [Fig. 2(a)]. The fact that the calculated increase in the dead layer from M_S values (~3.9 nm) is higher than that obtained from the $Mn^{4+}/Mn^{3+/4+}$ ratio (~1.5 nm) suggests that nonferromagnetic phases, accounting for the observed drop of $Mn^{3+/4+}$ intensity, contribute to diminish M_S. On the other hand, the (110) spectra evidence a main $Mn^{3+/4+}$ line unaffected by the STO capping, and they do not present any Mn^{4+} resonant line, suggesting that no further change in the electronic state of Mn in the (110) electrodes is induced by the STO capping layer.

To study the interface valence states, we performed XPS experiments on bare electrodes and 2 nm STO capped ones. Figure 4 shows the resulting Mn $2p$ photoemission spectra. The binding energy in both electrodes as well as the splitting is the same as that expected for an intermediate state $Mn^{3+/4+}$,[15] thus indicating that within the experimental conditions for detection (45° grazing incidence) similar Mn electronic states are expected in the last LCMO unit cells. In the case of the spectra from capped electrodes, we observe a shift of the core levels towards lower binding energy. The origin of this energy shift can be attributed to a change in the overall charge on the Mn ion, with reduced Mn sites.[6] Moreover, in the (001) capped electrode another contribution marked by an arrow appears at ~5 eV of the Mn $2p_{3/2}$ peak, likely to be a shake up peak related to the presence of Mn^{2+} ions.[16] On the other hand, (110) capped electrode spectrum does not present evidence of this secondary contribution.

In summary, we have observed that LCMO electrodes and STO capped ones grown on (001) and (110) STO substrates display different magnetic properties with different sensitivities to capping layers. For the (001) electrodes, we notice a reduction of the magnetic properties (M_S) and an increase of the electronic phase separation in the capped electrode. Also, the charge modification of the Mn ion located at the STO layer/LCMO interface is evidenced in the (001) capped electrodes. The better magnetic and electronic properties of the (110) electrodes and interfaces make them a suitable alternative to the (001) ones for spintronics devices.

Financial support by the MEC of the Spanish Government (Project No. NAN2004-9094-C03, MAT2005-5656-C04, and NANOSELECT CSD2007-00041), by the European Community (project MaCoMuFi (FP6-03321) and FEDER), by the Ministry of Sciences and High Education of the Polish Government (Project No. 1 P03B 123 30), and the CSIC (Project No. 2006PL0021) is acknowledged.

[1] Y. Lu *et al.*, Phys. Rev. B **54**, R8357 (1996).
[2] M. Viret *et al.*, Europhys. Lett. **39**, 545 (1997).
[3] M.-H. Jo *et al.*, Phys. Rev. B **61**, R14905 (2000).
[4] V. Garcia *et al.*, Phys. Rev. B **69**, 052403 (2004).
[5] H. Kumigashira *et al.*, Appl. Phys. Lett. **88**, 192504 (2006).
[6] J.-L. Maurice *et al.*, Philos. Mag. **86**, 2127 (2006).
[7] A. Ruotolo *et al.*, Appl. Phys. Lett. **88**, 252504 (2006).
[8] I. C. Infante *et al.*, J. Appl. Phys. **101**, 093902 (2007).
[9] I. C. Infante *et al.*, Phys. Rev. B, **76**, 224415 (2007).
[10] P. Panissod *et al.*, Phys. Rev. B **63**, 014408 (2001).
[11] L. Brey, Phys. Rev. B **75**, 104423 (2007).
[12] M. Bibes *et al.*, Phys. Rev. Lett. **87**, 067210 (2001); M. Bibes *et al.*, Phys. Rev. B **66**, 134416 (2002).
[13] A. A. Sidorenko *et al.*, Phys. Rev. B **73**, 054406 (2006).
[14] J. P. Renard and A. Anane, Mater. Sci. Eng., B **63**, 22 (1999).
[15] M. Oku *et al.*, J. Electron Spectrosc. Relat. Phenom. **7**, 465 (1975).
[16] E. Beyreuther *et al.*, Phys. Rev. B **73**, 155425 (2006).